Proceedings of the ASME 2022
International Mechanical Engineering Congress and Exposition
IMECE2022
October 30–November 3, 2022, Columbus, OH

IMECE2022-95871

LOCAL IOT WIRELESS NETWORK FOR ROAD SURFACE TEMPERATURE MODELING AND FORECASTING USING DEEP LEARNING METHODS

Andrew C. Grizzle[1], Dr. Timothy Oladunni[2], Dr. Sasan Haghani[2]

[1]Mechanical Engineering Dept., University of the District of Columbia, Washington D.C., U.S.
[2]Electrical Engineering Dept., University of the District of Columbia, Washington D.C., U.S.

ABSTRACT

Winter road safety procedures are crucial for maintaining safe operating conditions and daily transportation activities without impedance or risk to the population. Typically, road surface salting mitigates ice build-up; however, road surface temperature (RST) forecasting with mathematical models performs poorly where the geographic location and climate cannot be generalized or described models trained with data from sensors in unrepresentative geographic locations. Additionally, modeling interactions among meteorological, geographical, and physical road characteristics can prove challenging. This study proposes using deep neural networks to model the nonlinear interactions of the above features, thereby creating a better model for forecasting RST by up to twelve hours into the future.

Keywords: IoT, deep learning, hyperparameter, recurrent neural network, deep neural network

1. INTRODUCTION

According to the U.S. Federal Highway Administration (USDOT FHWA, 2017), snowfall and icing on road surfaces accounted for 136,309 casualties and 1,836 deaths that year during winter. Consequently, responders have proactively implemented various road maintenance procedures to prevent road surface icing. In most cases, mathematical models have provided road surface temperature (RST) predictions, which are generally incorrect estimates of an RST variation model, mainly due to non-linear interactions and relationships among complex geographical and meteorological factors. This project's first objective is to conduct a performance comparison of two deep learning models for short and medium-term multi-variable predictions. The input data are time series of the global horizontal irradiance (GHI), ambient air temperature, and barometric pressure, with the response data being RST. This investigation focuses on three models - Deep Neural Network (DNN), Convolutional Neural Network (CNN), and a specific type of Recurrent Neural Network (RNN): Long Short-Term Memory (LSTM). Previous studies showed that deep neural networks, particularly LSTM models, performed well when forecasting multivariate weather-dependent Wind Power Generation [1] and Solar Irradiance [2]. The contribution of this project is to implement, evaluate and compare these three models for multivariate analysis and prediction, which is to capture the influence of multiple variables on the target variable. The standard DNN will benchmark the performance of the deep learning models. The second objective is to implement an Internet of Things (IoT) wireless sensor network (WSN) system. The WSN system will be deployed outdoors for an extended time receiving, logging, and transmitting climatological data and road surface temperature, which will train the deep learning algorithms. Therefore the sensor node electronics and WSN system must be configured to achieve continuous data collection with low power consumption.

1.1 Methodology

Data was collected every 10 seconds over the WSN network. Typically a WSN network consists of the End Device/sensors, Router, and Coordinator; however, this study only utilized two wireless communication modules to create a network consisting of the End Device and coordinator. The data were normalized ("Fig. 1") to accommodate the sigmoid and hyperbolic tangent activation function limits between zero and one. An added benefit is faster model training and performance.

1.2 IOT - Hardware Specification

Air Temperature, Humidity, Barom. Pres. Integrated into a single board, the BME280, "Fig. 2", is an environmental sensor that includes a temperature sensor, a humidity sensor, and a barometer. It features excellent accuracy, many functionalities, and a tiny footprint, among other characteristics. The sensor has a temperature inaccuracy of 0.5 $^{\circ}C$ and a relative humidity error of 2%. When operating within the detection temperature range, it exhibits notably steady performance. Furthermore, the offset

Documentation for `asmeconf.cls`: Version 1.30, April 28, 2022.

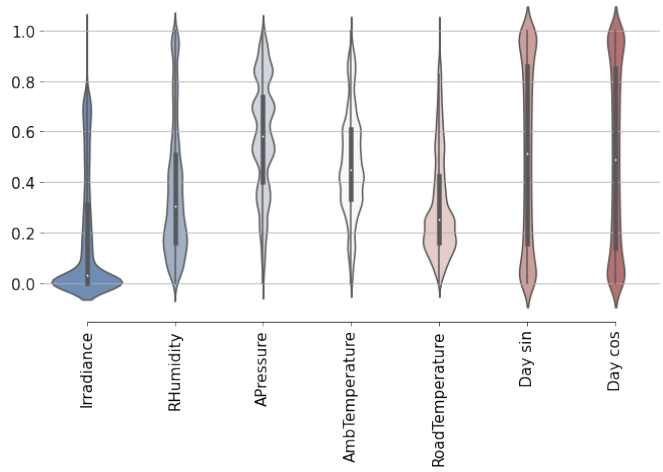

FIGURE 1: DATA NORMALIZATION BETWEEN ZERO AND ONE.

temperature coefficient is 1.5 $Pa \cdot K^{-1}$, equivalent to 12.6 cm at a 1 degree Celsius temperature shift.

FIGURE 2: BME280 ENVIRONMENTAL SENSOR MODULE.

Road Surface Temperature, "Fig. 3". The MLX90614 is an infrared thermometer that measures temperature without physical contact. The TO-39 container conveniently packages the IR-sensitive thermopile detector chip and signal conditioning ASIC. The thermometer is factory calibrated and has two different output methods: PWM and SMBus (i.e., TWI, I2C). Regarding temperature resolution, the 10-bit PWM output has a precision of $0.14°C$, and the TWI interface boasts a resolution of $0.02°C$. Regarding temperature ranges, the MLX90614 is factory calibrated in a broad range: -40 to $85°C$ and -70 to $382.2°C$ for ambient temperature and object temperature, respectively. The temperature value measured is the average of all items inside the sensor's Field Of View. The MLX90614 has a standard accuracy of $0.5°C$ at ambient temperatures, which is excellent.

Solar Irradiance Meter. Sun photovoltaic cells, "Fig. 4", are a cost-effective and dependable method of determining solar irradiance data. As it is a photoelectric device, exposing it to sunlight generates a potential (voltage) across the material. Internally, the device is a single junction P-N Semiconductor that operates according to specific I-V curve rules. Solar photovoltaic cells have four critical terms: open-circuit voltage (V_{OC}), short-circuit current (I_{SC}), maximum operating voltage (V_{MP}), and maximum

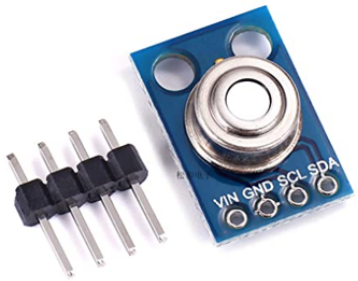

FIGURE 3: MLX90614 INFRARED THERMOMETER.

operating current (I_{MP}). The value of the I_{SC} is proportional to the intensity of sunlight. Therefore the solar Irradiance value is inferred based on the current I_{SC} value in comparison with the solar cell's calibrated I_{SC} value at 1000 $W \cdot m^{-2}$.

FIGURE 4: CALIBRATED SOLAR CELL.

Xbee Radio. "Fig. 5". Wireless communication between end-point devices in a WSN is accomplished through the usage of the Xbee protocol. Xbee is a radio communication module manufactured by Digi that is compatible with the ZigBee, 802.15.14, and other protocols. The Xbee works at a frequency of 2.4 GHz and ranges between 10 and 30 meters.

Arduino Uno Board. Arduino, "Fig. 6", is a microcontroller system that is free and open-source, and it is based on a simple input-output board. Arduinos are often used for prototyping and constructing standalone interactive items [**?**] and for developing embedded software. Arduino was created to be simple to understand and use, versatile, and dependable, among other things. They are commonly employed as portable devices in wireless sensor networks [**?**], which is a common application. There are a variety of sensors and actuators that are compatible with the Arduino platform. Typical actuators include popular sensors such as temperature and light sensors (as noted above) and sound sensors and speakers. Other basic actuators include LEDs and digital and analog outputs.

1.3 Deep Learning - Models

Because the deep learning algorithms were built in Python and used the TensorFlow backend, we created code scripts to

FIGURE 5: XBEE-S2C WIRE ANTENNA.

FIGURE 6: ARDUINO UNO R3.

test and execute simplified versions of the deep learning models. Additionally, we used Google's Colab python notebook, which gives an online Python environment and complimentary access to a GPU for expedited Deep Learning model training. In this work, we utilize three different types of models. The first model is a Deep Neural Network (DNN), which serves as a benchmark for the rest of the models. Secondly, a Convolutional Neural Network (CNN) is used to compare with a third model, which is a form of Recurrent Neural Network (RNN) known as a Long Short-Term Memory (LSTM).

Dense Neural Network. Derived from artificial networks (ANNs), the DNN is a type of ANN built with multilayers architecture ("Fig. 8") that can reconstruct raw data sets from their original features to their learned features. This means that instead of selecting features manually [**?**], users can "learn" features from neural networks (NNs), which will result in increased accuracy and more generalization with the taught features.

Convolutional Neural Network. A CNN is an ANN designed to analyze spatial data and is frequently used for image and video processing. The neurons of the CNN are arranged like that of multilayer perceptrons that have been regularized. Among the layers that make up a CNN are an input layer, an output layer, and a hidden layer that contains several convolutional layers and pooling layers, fully connected layers, and normalizing layers. With the removal of constraints and improved image processing efficiency, we have a considerably more effective system that is easier to train for image processing and natural language processing. In our study, we utilize a one dimensional CNN model to analyze the time-series data, "Fig. 9".

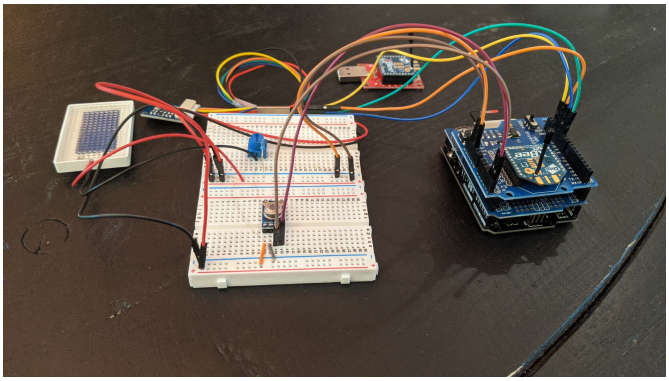

FIGURE 7: ASSEMBLED WSN.

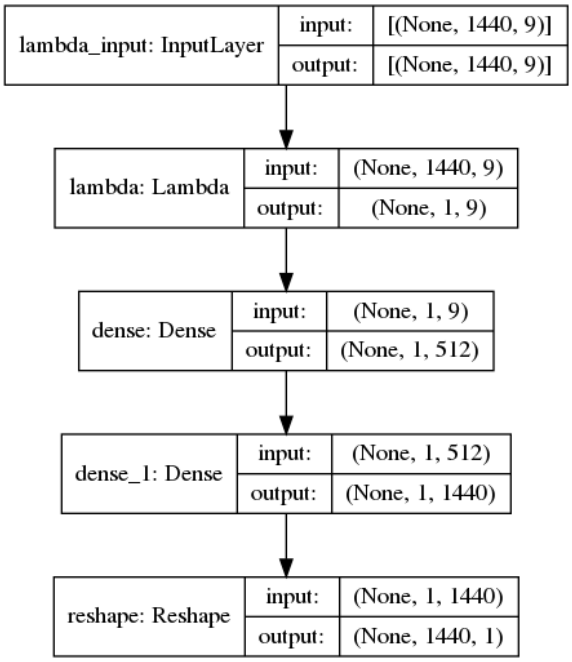

FIGURE 8: ARCHITECTURE OF DNN IN THIS STUDY.

Long Short-Term Memory. "Fig. 10". The accuracy and universality of the RST forecast can be improved by using an LSTM model, which is proposed in this paper. When used in conjunction with backpropagation across time, the LSTM network effectively eliminates the vanishing and expanding gradient problems in machine learning. It features segments that make it "smarter" than a typical neuron, and it has a memory for recent sequences that other blocks may access.

1.4 Evaluation of Model Performance

The mean absolute error (MAE), a coefficient, is used in this study to evaluate the forecasting results of the three models. MAE calculates the average magnitude of errors in a group of predictions without taking their direction into account. It is the average of the absolute differences between prediction and actual observation over the test sample, where all individual deviations are given equal weight. The MAE value is between 0 and infinity. A model with an MAE value near zero is more capable of

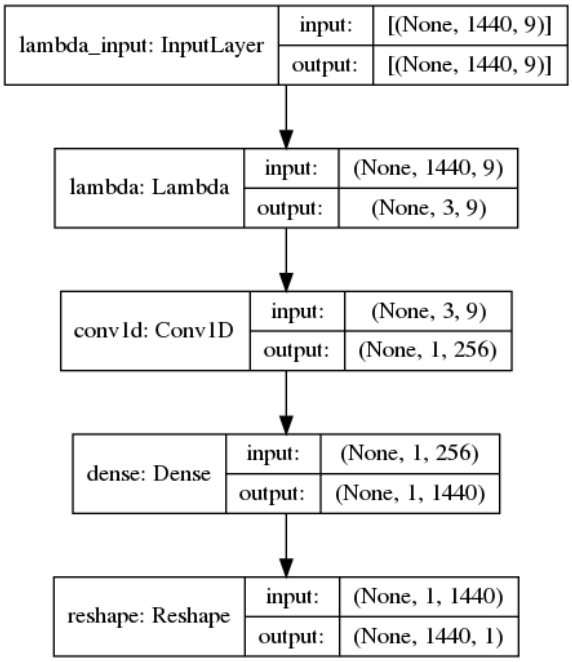

FIGURE 9: ARCHITECTURE OF CNN IN THIS STUDY.

producing accurate projections. The equation below is used to determine MAE.

$$MAE = \frac{1}{n}\sum_{j=1}^{n}|y_j - \hat{y}_j| \tag{1}$$

where n is the number of samples, y_j is the target output and $\hat{y}_j$ is the model output.

1.5 Hyper-parameter tuning

Optuna [**?**] was used to tune the models. The results of the hyperparameter tuning of the LSTM model are below. The hyperparameter data from the other models are in the supplemental section and can be accessed upon reasonable request.

2. RESULTS AND DISCUSSION

2.1 Climatological Data

"Fig. 12" shows a plot of the captured data, from 11th to the 30th of May. Plots of the RST show some noise but overall have a low signal-to-noise ratio.

"Fig. 13" shows the Pearson correlation coefficient between the measured variables and target. RST shows strong correlation between Irradiance and ambient air temperature. Relative humidity appears to be negatively correlated with RST. The equation to calculate the Pearson correlation coefficient is shown below.

$$r = \frac{\sum(x_i - \bar{x})(y_i - \bar{y})}{\sqrt{\sum(x_i - \bar{x})^2 \sum(y_i - \bar{y})^2}} \tag{2}$$

where x_i, y_i is the values of the x-variable and y-variable in the sample, $\bar{x}, \bar{x}$ is the mean of the values of the x-variable and y-variable respectively.

The seasonal and trend data plots in "Fig. 14a" and "Fig. 14b" is graphed by plotting the average values over the given time period, twenty four hours and 3 months respectively. As shown

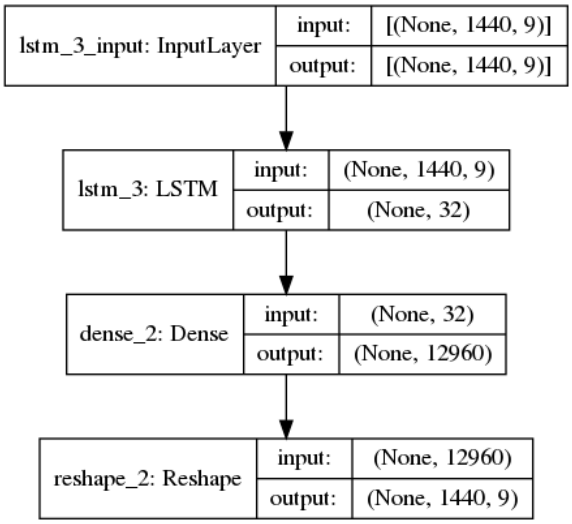

FIGURE 10: ARCHITECTURE OF LSTM IN THIS STUDY.

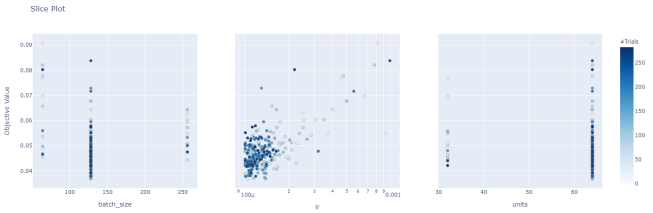

(a) Batch size, learning rate, and number of units hyperparamter optimization.

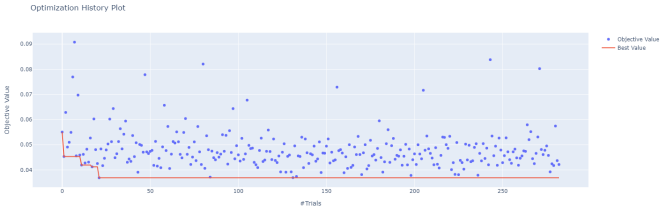

(b) Optimization history plot.

in "Fig. 13", there is strong corrrelation between RST and Irradiance. The RST value seems to have slight time lag, which is expected as RST general increases in temperature with increased solar radiation exposure. With the exception of Ambient pressure and relative air humidity, the trend of the data increases at varying rates. Between the months of May and July as summer weather becomes prevalent, ambient temperature and solar radiation flux increases.

2.2 Model Performance.

"Fig. 14a" shows the RST forecast 12hrs into the future, given the past twelve hours of data. There is a relatively equal performance between All three models. In general, the models struggle to predict the higher-frequency changes in RST temperature, which is expected, considering that the models have relatively simple architecture and parameters. Additionally, the models' output is "single shot" vector representations of the forecasted RST, producing less accuracy with longer forecasting win-

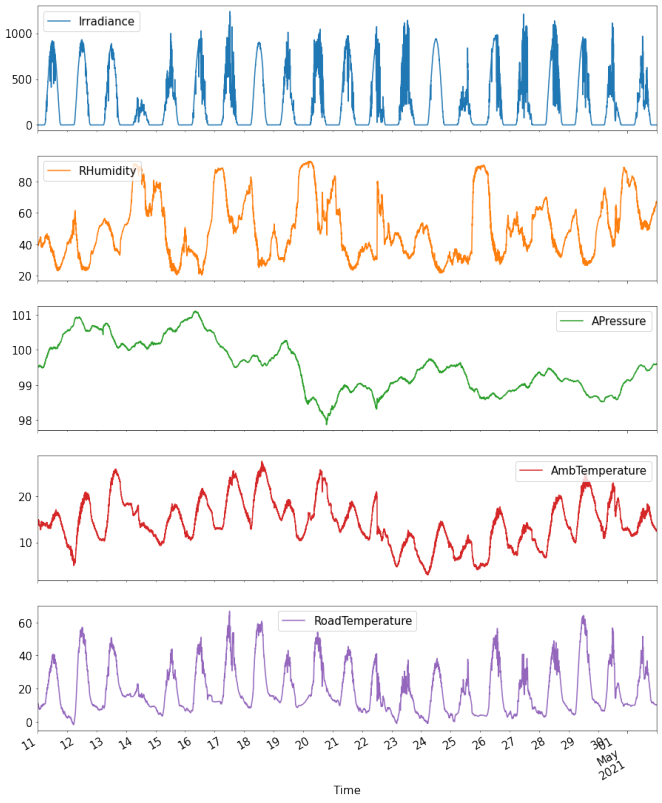

FIGURE 12: PLOT OF CLIMATOLOGICAL AND RST DATA.

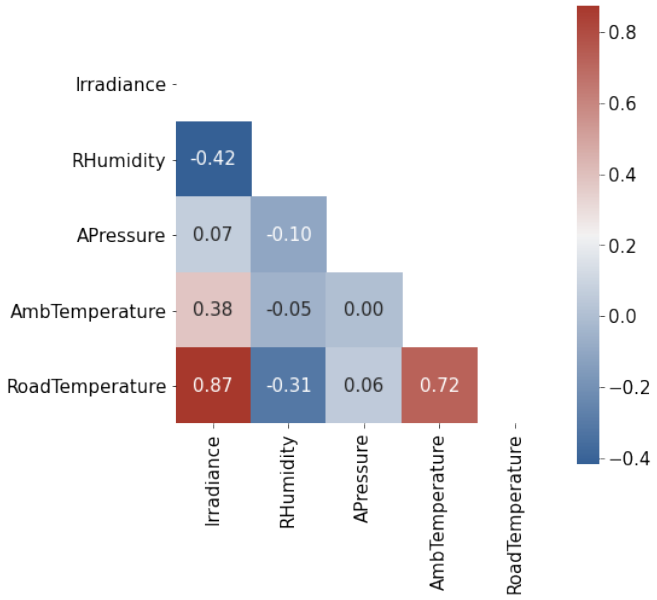

FIGURE 13: CORRELATION MAP OF RST WITH CLIMATOLOGICAL DATA.

dows. The MAE values are shown in "Fig. 15d", and are of the normalized variables.

3. CONCLUSION

A deployed WSN network successfully collected meteorological and RST data. Data was collected for approximately 2.5 months and modeled using three ANN models. All three models successfully forecasted within twelve-hour windows at less than 0.02 MAE (of normalized data between 0 and 1). The LSTM model proved to be better at generalizing by scoring less than 0.012 MAE. One major limitation was the absence of a rain meter since rain significantly affects the RST and directly contributes to icing events.

ACKNOWLEDGMENT

This research is supported by the Lockheed Fellowship Program and the National Science Foundation-CREST Award (Contract # HRD- 1914751) and the Department of Energy/ National Nuclear Security Agency (DE-FOA-0003945).

REFERENCES

[1] Mishra, Sambeet, Bordin, Chiara, Taharaguchi, Kota and Palu, Ivo. "Comparison of deep learning models for multivariate prediction of time series wind power generation and temperature." *Energy Reports* Vol. 6 (2020): pp. 273–286.

[2] Wojtkiewicz, Jessica, Hosseini, Matin, Gottumukkala, Raju and Chambers, Terrence Lynn. "Hour-ahead solar irradiance forecasting using multivariate gated recurrent units." *Energies* Vol. 12 No. 21 (2019): p. 4055.

[3] Banzi, Massimo. "Getting Started with Arduino (Make: Projects)." (2008).

[4] Faludi, Robert. *Building wireless sensor networks: with ZigBee, XBee, arduino, and processing*. " O'Reilly Media, Inc." (2010).

[5] Wang, Xizhao and He, Qiang. "Enhancing generalization capability of SVM classifiers with feature weight adjustment." *International Conference on Knowledge-Based and Intelligent Information and Engineering Systems*: pp. 1037–1043. 2004. Springer.

[6] Akiba, Takuya, Sano, Shotaro, Yanase, Toshihiko, Ohta, Takeru and Koyama, Masanori. "Optuna: A next-generation hyperparameter optimization framework." *Proceedings of the 25th ACM SIGKDD international conference on knowledge discovery & data mining*: pp. 2623–2631. 2019.

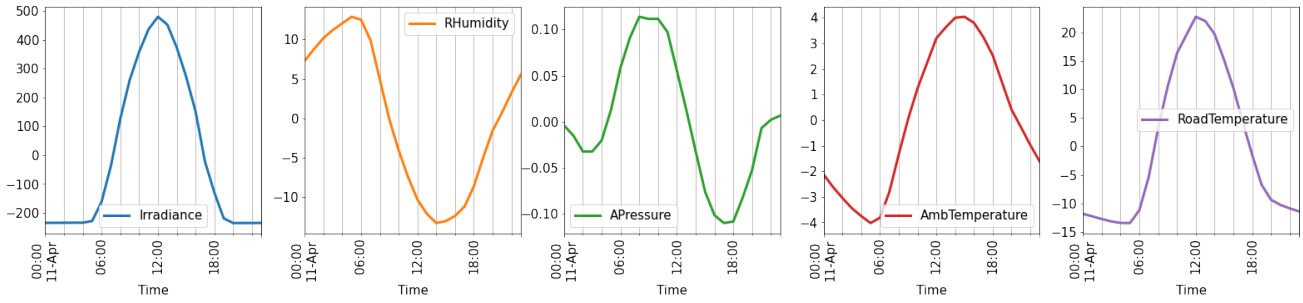

(a) Seasonality of data over 24hrs.

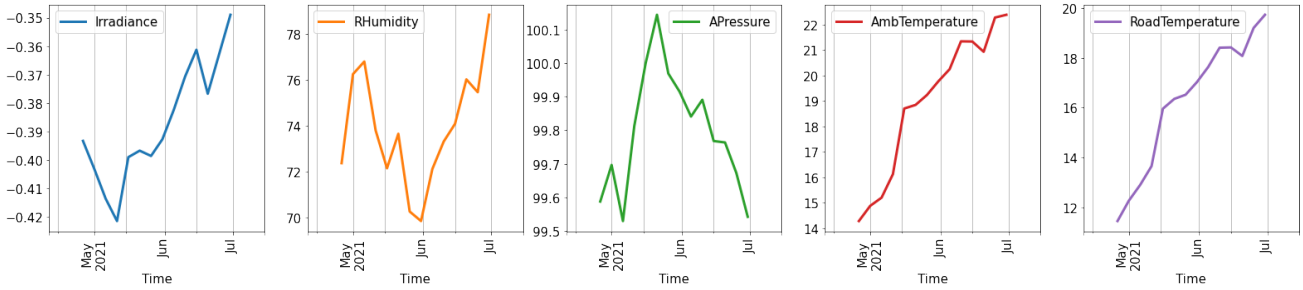

(b) Trend of data over duration of study.

FIGURE 14: SEASONALITY AND TREND ANALYSIS.

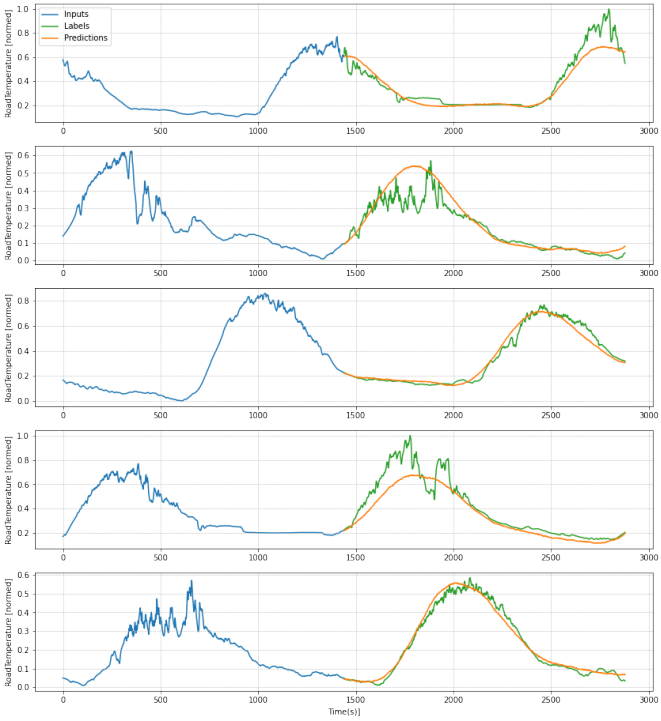

(a) DNN forecast.

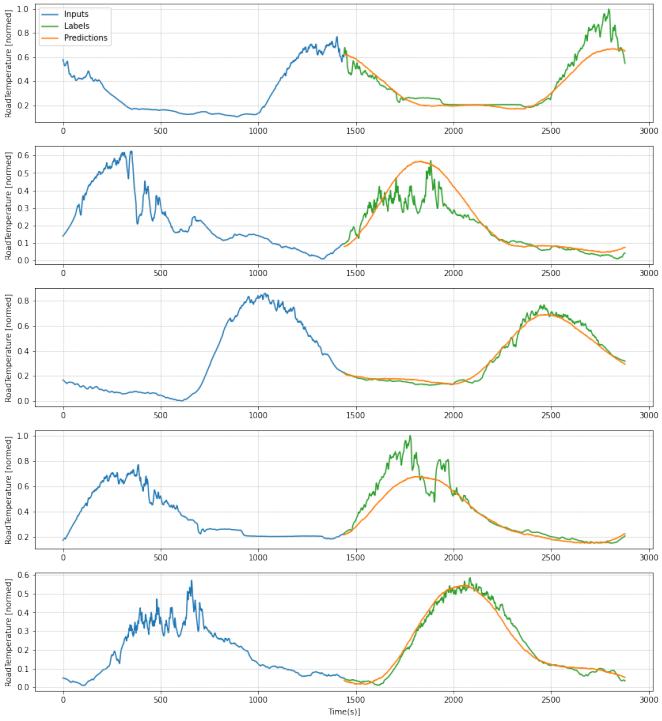

(b) CNN forecast.

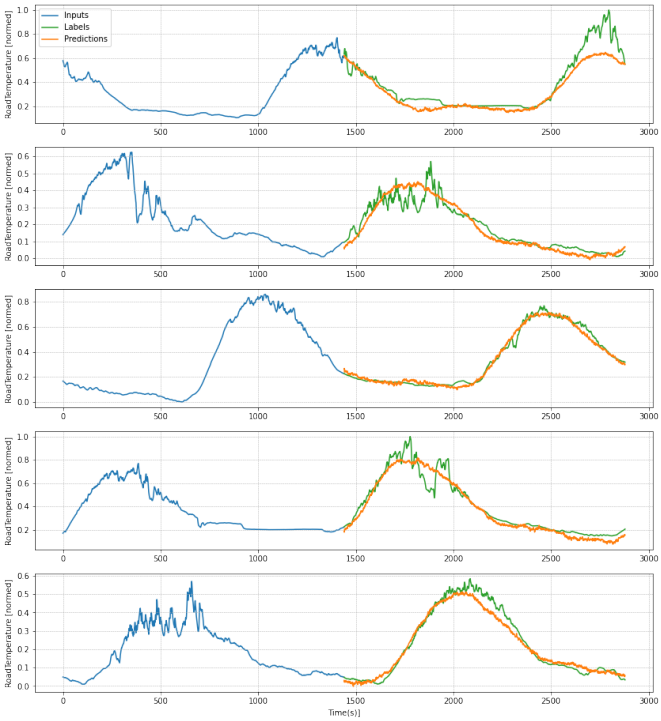

(c) LSTM forecast.

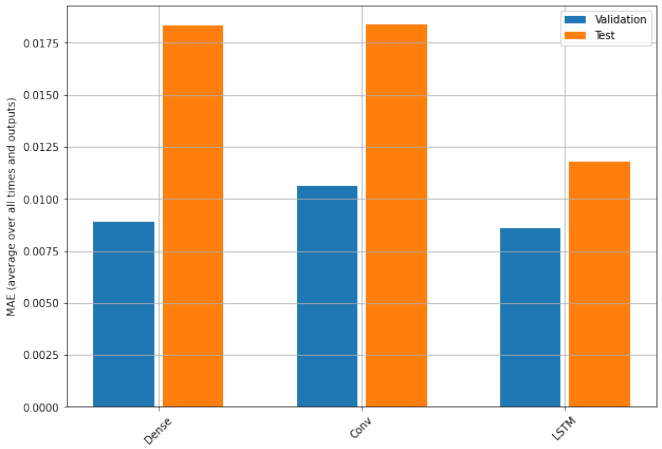

(d) MAE of models.

FIGURE 15: MODEL FORECASTING PERFORMANCE.